

# DIVERGENCE AND VORTICITY AT SOLAR MESOGRANULAR SCALES

W. PÖTZI<sup>1</sup>, P. N. BRANDT<sup>2</sup>

<sup>1</sup>*Observatorium Kanzelhöhe, Universität Graz,  
A-9521 Treffen, Austria*

<sup>2</sup>*Kiepenheuer-Institut, Schöneckstr. 6,  
D-79104 Freiburg, Germany*

**Abstract.** Ten time series of solar granulation filtergrams at high spatial resolution and various durations, i. e. from 20 min to several hours, (one data set is from numerical simulations) are used to investigate the relation between vorticity and divergence at meso granular scales. Velocity fields at various scales were generated by local correlation tracking (LCT) and from these divergence and vorticity were computed. In all data sets we find a strong preference of stronger vortices at downflowing regions, i.e. where the divergence is negative. This holds especially for scales larger than granular sizes and for longer lifetimes.

**Key words:** granulation - meso granulation - vorticity - divergence

## 1. Introduction

Space observations of the solar surface show Doppler velocities at all spatial scales between the granulation and giant cells (Hathaway *et al.*, 2000). Although not clearly separated from granulation on the one hand and from supergranulation on the other hand, the meso granulation – first described by (November *et al.*, 1981) – represents a clearly visible but not well understood phenomenon. Various techniques had been used to investigate and visualize it: velocity maps established with LCT (local correlation tracking) methods (November *et al.*, 1987; Brandt *et al.*, 1991; Muller *et al.*, 1992; Roudier *et al.*, 1998), dopplergrams (November *et al.*, 1981; Wang *et al.*, 1989; Deubner, 1989), or spectral time series (Straus *et al.*, 1992; Straus and Bonaccini, 1997). Brandt *et al.* (1991) showed that granules of certain types tend to be located preferentially in different meso granular regions. Pötzi *et al.* (2003) found a correlation between granular types and

the divergence pattern - fragmenting and exploding granules were located at positive divergence regions whereas fading granules showed a tendency to occur in regions of negative divergence. Using three time series Pötzi and Brandt (2005) could show that vortices are stronger in inflows without any preference of the rotational direction; to some extent the present investigation is a continuation of this previous work. Wang *et al.* (1995) studied Pic du Midi time series and found "that vorticities seem to have a closer association with inflows than outflows". In numerical simulations Zirker (1993) found very strong vortices in intergranular lanes and also Stein and Nordlund (1998) could show that most of the vortices are located outside the granules. In theoretical computations of the horizontal divergence-vorticity correlation Rüdiger *et al.* (1999) found a small but always negative value for the northern hemisphere – with a large scatter, however.

## 2. The Data

For our investigation we used ten high resolution data sets of solar granulation images from 5 instruments; they are of various durations and were observed at different locations on the Sun (see Tab. I).

- 6 data sets originate from the Dutch Open Telescope (DOT) at a resolution of 14 pixel per arcsec and a time lag between single frames of 20 to 30 seconds. These data sets are mostly from quiet Sun regions, one is below a filament and one near AR 9669. The first three data sets are near disc center, the last two ones are 45 degree north and south, respectively. All of these data sets were speckle-reconstructed and  $k$ - $\omega$  filtered. The data are available to the public at <http://dotdb.phys.wu.nl/DOT/>.
- One data set is from the old Swedish telescope of 45 cm aperture; this data set has a lower resolution than most of the other data sets but it has the longest duration. This data set was destretched for atmospheric distortion and  $k$ - $\omega$  filtered. More details can be found in Simon *et al.* (1994).
- From the new Swedish telescope of 100 cm aperture we got one data set – this data has the highest resolution and it was reduced with a Multi-Object Multi-Frame Blind Deconvolution procedure (van Noort *et al.*, 2005).

**Table I:** *SVST 45/100*: Old and new Swedish Telescope at La Palma of 45 cm and 100 cm aperture. Type: *QS*= quiet Sun; *AR*= active region 9669; *Fil.*= below filament.

Data set (date)	Instrument	Resol. (pix/")	Length (min)	$\Delta t$ (sec)	Position ( $\mu$ )	Type
1993-06-25	SVST 45	8	347	21	0.97	QS
Model <sub>Ludwig</sub>	Model	7	61	20	1.00	QS
2001-10-19	DOT	14	96	30	0.92	AR
2003-06-16	DOT	14	57	20	1.00	QS
2004-08-22	SVST 100	25	78	14	1.00	QS
2005-09-14	DOT	14	42	30	0.91	Fil.
2005-10-04	VTT	20	18	10	1.00	QS
2005-10-19	DOT	14	68	30	0.98	QS
2006-06-04	DOT	14	35	30	0.70	QS
2006-07-26	DOT	14	58	30	0.66	QS

- From the German VTT we got the shortest set; however, it has a very high resolution and quality; this set was also speckle-reconstructed.
- Additionally to the observed data we used a series of numerical simulations of solar convection; due to calculation time and memory restrictions this data set is of lower resolution, which, however, to some extent is compensated by the missing atmospheric degradation.

### 3. Methods

**Velocities:** Velocities have been obtained via local correlation techniques (LCT, November *et al.* (1987)). This method has one drawback: The LCT method calculates the correlation for shifts of one pixel in each direction; if the time step between two images is very long and the resolution is very high this method has to extrapolate displacement values. That means there exists a velocity  $v_0$  above which each value has to be extrapolated:

$$v_0 = \frac{730 \text{ km}}{\text{Resol.} * \Delta t}.$$

In case of DOT data:  $v_0 = 730/(14 * 30) = 1.74$  km/s, i.e. velocities higher than this value are uncertain. We have tested all velocity fields for extrapolated values. For mesogranular scales the subfields are large enough that extrapolations only occur at image borders, which are not taken into account for our calculations.

**Divergence and Vorticity:** In physical terms, the divergence of a vector field is the extent to which the vector field flow behaves like a source or a sink at a given point. Indeed, an alternative, but logically equivalent definition, gives the divergence as the derivative of the net flow of the vector field across the surface of a small sphere relative to the surface area of the sphere. If the divergence is positive – a source – the matter is coming from somewhere inside the region of interest, in the case of the solar atmosphere the matter must come from lower layers, i.e. matter is flowing upwards. The opposite holds for a sink.

In simple words, vorticity is the rotation of a vector field. A positive vorticity value indicates a counter-clockwise rotation of the vector field. For a 2-D velocity field the divergence and the vorticity are defined as:

$$div(\vec{v}) = \nabla \vec{v} = \frac{\partial \vec{v}_x}{\partial x} + \frac{\partial \vec{v}_y}{\partial y}, \quad vort(\vec{v}) = \nabla \times \vec{v} = \frac{\partial \vec{v}_y}{\partial x} - \frac{\partial \vec{v}_x}{\partial y}.$$

**Coriolis force:** In any rotating system we have to deal with the Coriolis force; the effect of this force can be estimated by the inverse of the Rossby number (Stix, 2004):

$$Ro = u/(2\Omega l).$$

This number is the ratio of inertia and Coriolis forces. Where  $u$  is the typical mesogranular velocity (some 100 m/s), the length  $l$  is the size of mesogranules (about 5 Mm), and  $\Omega$  is the rotation rate of the Sun. In our case  $Ro$  is about 10, i.e. for a latitude of 45 degrees the value of the velocity due to the Coriolis force is 25 to 35 m/s.

**Visualization** The vorticity and the divergence are calculated from each data series at different spatial resolutions, that means that in principle the LCT is performed at different resolutions by applying subwindows of different sizes. E.g. when a subwindow of 8 pixels is used for the LCT the velocity vectors are smoothed over an area of about 8x8 pixels; due to the LCT method it is not possible to calculate vectors for each individual pixel, because this method compares locations of small subwindows in order to obtain their proper motion. For a distinction between the different regimes

DIVERGENCE AND VORTICITY AT SOLAR MESOGRANULAR SCALES

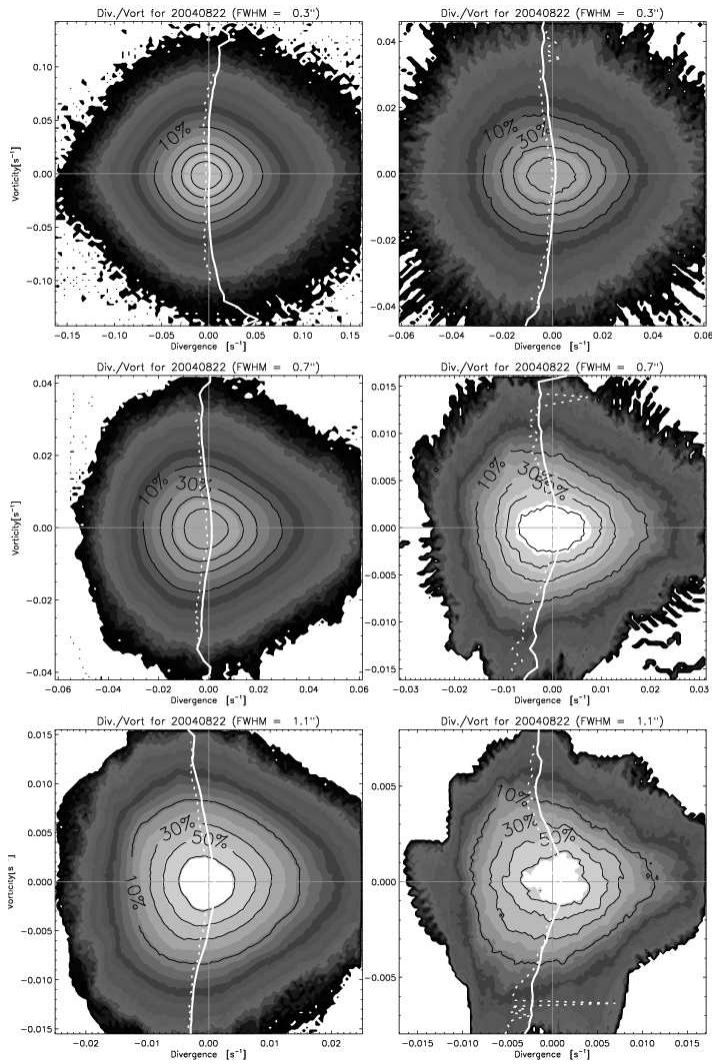


Figure 1: 2-D histograms for the VTT series at different LCT resolutions. The resolution changes from top to bottom from  $0''.3$  to  $0''.7$  and to  $1''.1$ . The smoothing window changes from 10 min on the left side to the full 78 min on the right side. The grey scale codes the number of values per bin. The solid and dotted lines in C-shape or anti C-shape are the mean values of divergence per vorticity bin and the maximum of the divergence per vorticity bin, respectively. Due to the asymmetric distribution of the divergence the contours assume an oval shape.

DIVERGENCE AND VORTICITY AT SOLAR MESOGRANULAR SCALES

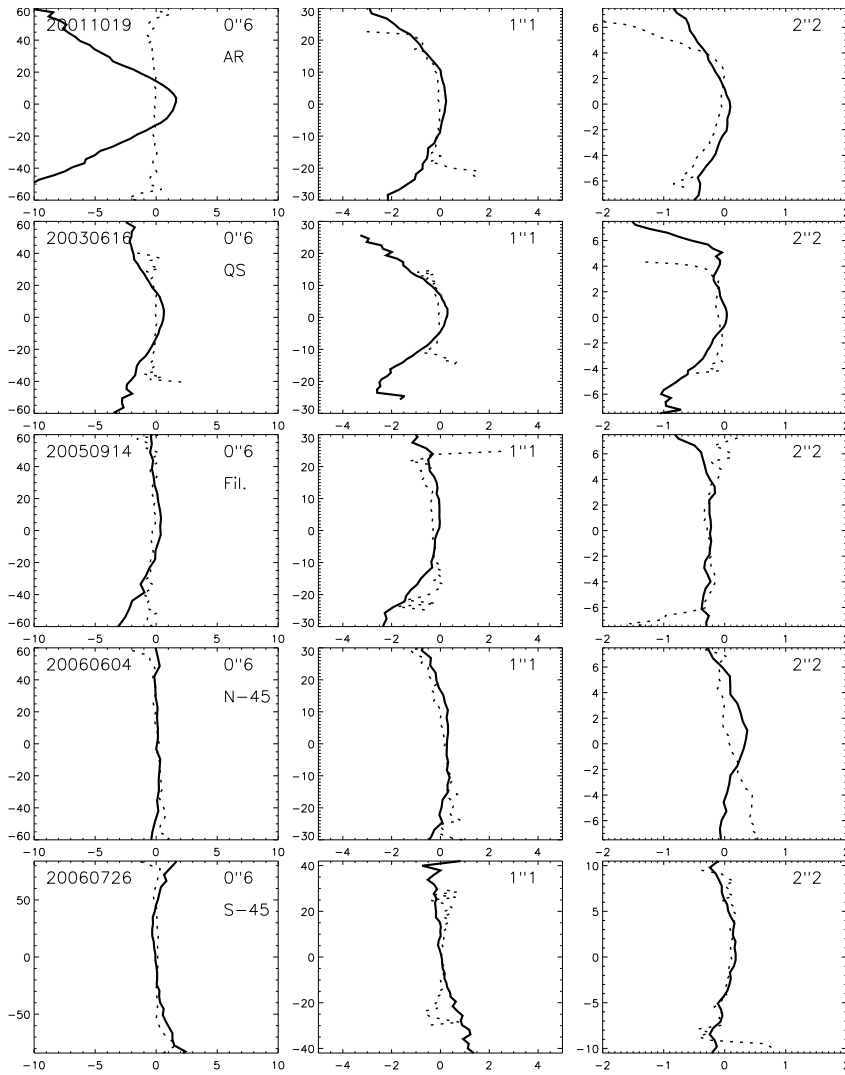


Figure 2: DOT data at three resolutions and at different positions on the solar disk. The solid line is the mean of the divergence for each vorticity bin and the dotted line is the same for rotatet data sets (see Sect. "Zero-Test" in text). The axes are the same as in Fig. 1, the axis scales are in units of  $10^{-3}/s$ . The divergence and vorticity values become smaller for larger LCT windows; both scales vary accordingly. For all sets the full time series was used with a temporal window of 20 minutes.

of motion, like granulation or mesogranulation, not only the spatial resolution has to be adjusted but also an averaging over a certain time span has to be applied to the divergence and vorticity maps. The granulation has a time scale of about 5 to 10 minutes. If the velocity or divergence maps are averaged over more than 10 minutes the pattern originating from granular motion begins to be smoothed out (Rieutord *et al.*, 2001). After more than 1 hour all of the granular motion is removed, the resulting maps show the behaviour of slower and larger motion regimes – the mesogranulation, and in case of averaging over more than 5 hours the supergranular pattern begins to appear. If the spatial resolution is high and the temporal averaging is long the pattern shows something like mesogranules disturbed by granules.

After the above steps a 2-D histogram is produced (see Fig. 1) with the divergence plotted along the x-axis and the vorticity along the y-axis. In this plot the number of values per histogram bin (which is a rectangle) is coded in grey-scale, otherwise a 3-D plot (surface-plot) would have to be generated. For a better visualization of the relation between the divergence and the vorticity the *mean divergence for a certain vorticity bin* is overplotted (bow-shaped curve). In the following plots only these mean divergence values are displayed. The total ranges for the vorticity and divergence are indicated by the ranges of the axes.

**Zero-Test:** In order to test and prove the significance of the results, we introduced a test. For this purpose we calculated the correlation between vorticity and divergence with rotated data, i.e. the vorticity is rotated against the divergence data by 90, 180, and 270 degrees and then we produced the same plots as above. In such a case the vorticity and the divergence should be uncorrelated and the mean values should therefore be 0, visible in our plots as a straight vertical line at the abscissa ( $x = 0$ ); this has been done for all data sets.

#### 4. Results

The plot in Fig. 2 refers to a large part of the DOT data. The first two rows show the typical behaviour, that was observed with almost all quiet Sun data sets observed at disk center. In the third row the inverted C-shape seems to be suppressed – may be due to the filament over the granulation. The last two rows are from 45 degrees north and south of the solar equator,

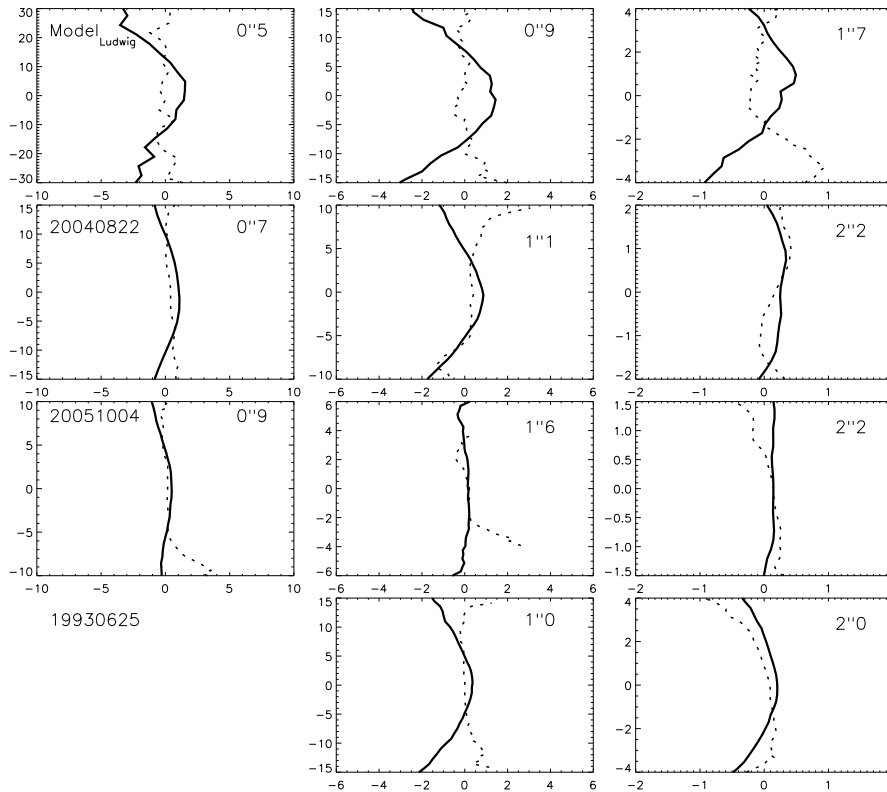


Figure 3: Data from different sources at three resolutions. For the last data set it was not possible to create velocity data at higher resolutions.

here the C-shape is very weak and only visible for the lowest resolution. In Fig. 3 the other data sets are plotted. They were all located at the disc center and in quiet regions. In these data sets the inverted C-shape is visible nearly everywhere except in the data from the VTT (3rd row).

## 5. Discussion

The effect that both positive and negative vortices seem to be located preferentially in regions of negative divergence can be seen at all scales and in nearly all data sets. Longer data sets show this effect much more clearly

than the short ones; this can be explained by the lifetime of the features taken into account – at mesogranular scales we have to integrate over a longer time (1 hour and more) in order to get rid of granular disturbances. Even near active regions and below a filament (Fig. 2, middle row) the effect is visible.

The deviation of the mean divergence at higher vorticity values means that in inflows the vortices become stronger than in the other regions; in other words, if plasma is sinking down it does so in vortices. This behaviour seems to hold for granulation and mesogranulation - it should also hold for supergranulation. Our results confirm earlier findings by Wang et al. (1995) but contradict the "small, but always negative, divergence-vorticity correlation" found by Rüdiger et al. (1999). In Fig. 7 of Stein and Nordlund (1998) the same effect was shown in numerical simulations, where the vorticity is concentrated in "downdrafts" outside of granule centers.

The two data sets observed at 45 deg north and south of the equator show a small and in the southern case even an opposite effect – if this is due to the Coriolis force it should be better visible at lower resolutions, because the factor  $l$  – the size of the elements – is increasing. The main problem with this data is the geometrical foreshortening of the images – for obtaining velocities these images have to be rescaled – thus they get smoother (loose spatial resolution) in the meridional direction. Therefore the accuracy is lower than in the other data sets. Nonetheless the southern data set shows the opposite behaviour at granular scales – this can, however, only be confirmed by additional data sets.

*Acknowledgements.* We thank Luc Rouppe v. d. Voort for supplying the SVST data, Hans-G. Ludwig for the model data, and Oskar v. d. Lühe for the VTT data. Special thanks go to Pit Sütterlin for his efforts in making the DOT data available to us at short notice.

## References

- Brandt, P. N., Greimel, R., Guenther, E., and Mattig, W.: 1991, *Lecture Notes in Physics* **m3**, 77–96.
- Deubner, F. L.: 1989, *Astron. Astrophys.* **216**, 259–264.
- Hathaway, D. H., Beck, J. G., Bogart, R. S., Bachmann, K. T., Khatri, G., Petitto, J. M., Han, S., and Raymond, J.: 2000, *Sol. Phys.* **193**, 299–312.

- Muller, R., Auffret, H., Roudier, T., Vigneau, J., Simon, G. W., Frank, Z., Shine, R. A., and Title, A. M.: 1992, *Nature* **356**, 322–325.
- November, L. J., Toomre, J., and Gebbie, K. B.: 1981, *Astrophys. J.* **245**, L123–L126.
- November, L., Simon, G. W., Tarbell, T. D., Title, A. M., and Ferguson, S. H.: 1987, *High Resolution Solar Physics II*, NASA CP-2483, pp. 121–127.
- Pötzi, W., Brandt, P. N., and Hanslmeier, A.: 2003, *Hvar Observatory Bulletin* **27**, 39–46.
- Pötzi, W. and Brandt, P. N.: 2005, *Hvar Observatory Bulletin* **29**, 61–70.
- Rüdiger, G., Brandenburg, A., and Pipin, V. V.: 1999, *Astronomische Nachrichten* **320**, 135–140.
- Rieutord, M., Roudier, T., Ludwig, H.-G., Nordlund, Å., and Stein, R.: 2001, *Astron. Astrophys.* **377**, L14–L17.
- Roudier, T., Malherbe, J. M., Vigneau, J., and Pfeiffer, B.: 1998, *Astron. Astrophys.* **330**, 1136–1144.
- Simon, G. W., Brandt, P. N., November, L. J., Scharmer, G. B., and Shine, R. A.: 1994, *Solar Surface Magnetism* pp. 261–270.
- Stein, R. F. and Nordlund, A.: 1998, *Astrophys. J.* **499**, 914–933.
- Stix, M.: 2004, *The Sun - An Introduction*, Springer, Berlin.
- Straus, T. and Bonaccini, D.: 1997, *Astron. Astrophys.* **324**, 704–712.
- Straus, T., Deubner, F. L., and Fleck, B.: 1992, *Astron. Astrophys.* **256**, 652–659.
- van Noort, M., van der Voort, L. R., and Löfdahl, M. G.: 2005, *Sol. Phys.* **228**, 191–215.
- Wang, Y.-M., Nash, A. G., and Sheeley, Jr., N. R.: 1989, *Science* **245**, 712–718.
- Wang, Y., Noyes, R. W., Tarbell, T. D., and Title, A. M.: 1995, *Astrophys. J.* **447**, 419–427.
- Zirker, J. B.: 1993, *Sol. Phys.* **147**, 47–53.